

Special
Collection

Calculation of Ionization, Excitation and Electron Capture Cross Sections for $\text{Be}^{4+} + \text{H}(2s, 2p)$ Collisions

Clara Illescas^{*[a]}

A computational study of $\text{Be}^{4+} + \text{H}(2s, 2p)$ collisions has been carried out employing the Classical Trajectory Monte Carlo (CTMC) method for the impact energy range from 20 keV/u to 1000 keV/u. The integral n partial cross sections for $\text{H}(n)$ excitation and $\text{Be}^{3+}(n)$ electron capture and, the total ionization and electron capture cross sections are calculated and

compared to recent semiclassical results. A general good agreement is observed for the n partial and total electron capture and ionization cross sections. The comparative study of the three inelastic processes show no significant differences between both excited targets.

Introduction

Collisions between hydrogen atoms and multiply charged ions play a fundamental role in tokamak plasmas. The diagnostics of impurity density and temperature in the plasma core is carried out by applying the Charge eXchange Recombination Spectroscopy (CXRS) technique.^[1] CXRS employs emissions from plasma impurities when a neutral beam of H atoms is injected and collides with the plasma ions A^{q+} . These collisions give rise to a charge exchange (also called electron capture (EC)) reaction that yields $\text{A}^{(q-1)+}$ into excited states. CXRS diagnostics requires accurate cross sections of the EC processes. In this sense, a recent work on Ar densities^[2] has pointed out the differences obtained from two sets of EC cross sections. Accurate data for atomic processes that involve the neutral beam particle also plays a key role in modelling the beam penetration into the plasma.^[3]

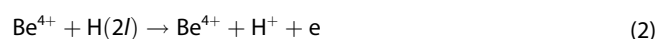
Be^{4+} impurity ions are expected to be found inside fusion reactors such a ITER because Be will be used as the armor material of the first wall, therefore the electron capture process may produce excited Be^{3+} ions. On the other hand, although the neutral beam injected is mainly composed of ground state atomic hydrogen, it is expected that as the beam penetrates, a fraction of atoms become excited. It is well known that cross sections for impurity ions colliding with excited H are larger^[4–6] than those for collisions with $\text{H}(1s)$, for this reason, contributions to the inelastic processes due to scattering on H in excited states have to be evaluated.

Although scattering cross sections for ion collisions with H ($n=2$) are required in the CXRS diagnostics, few theoretical works have considered collisions with excited hydrogen targets. In particular, collisions with Be^{4+} projectiles have been studied under the molecular orbital close-coupling (MOCC),^[7] atomic orbital close-coupling (AOCC),^[8,9] wavepacket convergent close-coupling (WP-CCC),^[10–12] the numerical solution of the time-dependent Schrödinger equation (GTDSE)^[13] and CTMC^[5,13–15] approaches. At the same time, and due to its toxicity, no experimental measurements in Be^{4+} collisions are available.

In this paper we consider fully stripped beryllium-ion collisions with $2l$ states of atomic hydrogen at energies between 20 keV/u and 1000 keV/u (fusion-relevant energies). We have applied the Classical Trajectory Monte Carlo (CTMC) method which is particularly useful at the so-called intermediate energy range where the inelastic processes (i.e. electron capture, ionization and excitation) are of comparable importance. In fact, at $E < 30$ keV/u, the most important process is the electron capture:



while ionization, which involves the removal of the target electron,



and the target excitation,



are processes that become dominant at $E > 30$ keV/u. We have addressed the study of these processes taking as a reference the recent semiclassical WP-CCC work of Antonio et al.,^[11] the only one that presents results of ionization and excitation,^[12] so our figures will focus on the comparison with the results of these authors.

Atomic units (a.u.) are used throughout unless otherwise stated.

[a] Dr. C. Illescas

Laboratorio Asociado al CIEMAT de Física Atómica y Molecular en Plasmas de Fusión, Departamento de Química, módulo 13, Universidad Autónoma de Madrid, Cantoblanco, 28049 Madrid (Spain)
E-mail: clara.illescas@uam.es

An invited contribution to a Special Collection dedicated to Pablo Villarreal Herrán on the occasion of his 70th birthday.

© 2023 The Authors. ChemPhysChem published by Wiley-VCH GmbH. This is an open access article under the terms of the Creative Commons Attribution Non-Commercial NoDerivs License, which permits use and distribution in any medium, provided the original work is properly cited, the use is non-commercial and no modifications or adaptations are made.

Computational Method

We use the Classical Trajectory Monte-Carlo method^[16] under the impact-parameter approximation,^[17] in which the internuclear position vector follows linear trajectories $\mathbf{R}=\mathbf{v}t+\mathbf{b}$, with relative nuclear velocity \mathbf{v} and impact parameter \mathbf{b} . The electronic motion is described classically by using a statistical ensemble of $N=2\times 10^6$ non-interacting particles,

$$\rho(\mathbf{r}, \mathbf{p}, t) = \frac{1}{N} \sum_{j=1}^N \delta(\mathbf{r} - \mathbf{r}_j(t)) \delta(\mathbf{p} - \mathbf{p}_j(t)) \quad (4)$$

which must satisfy the Liouville equation for the fixed-nuclei electronic Hamiltonian, with \mathbf{r} and \mathbf{p} electron position and momentum vector, respectively, with respect to the target nucleus. The ensemble of electron trajectories $\{\mathbf{r}_j(t), \mathbf{p}_j(t)\}$ are solutions of the Hamilton's equations.

The accuracy of the CTMC method strongly relies on the choice of the initial distribution.^[18–21] This method is commonly applied using the so-called microcanonical distribution,^[6,16,22,23] in which all electron trajectories have the same energy, ε . This classical description of the $H(n=2)$ orbital implies a cut-off of the spatial distribution at $r_0 = -Z_T/\varepsilon \sim 8$ a.u., so the tail of the quantal distribution for $r > r_0$ corresponds to classically forbidden trajectories (see Ref. [14]). To offset this deficiency, we have implemented the original idea of Hardie and Olson^[24] by constructing a hydrogenic initial distribution for the first excited state $H(n=2)$, as a linear combination of N microcanonical distributions with different energies:

$$p^h(r, p) = \sum_k^N a_k \rho_k^m(r, p) \quad (5)$$

with $N=8$ and whose weights, a_j (see Table 1), were calculated so as to achieve good approximations to the spatial and momentum quantal densities, together with the condition that the average energy, $\langle \varepsilon \rangle = \sum_{j=1}^m a_j \varepsilon_j = \varepsilon$, is equal to that of the corresponding quantum level ($\varepsilon = -0.125$ hartree). It is also ensured that the distributions included in the combination fulfill the conditions:^[22,25]

$$[(n-1/2)(n-1)n]^{1/3} < n_k \leq [(n+1/2)(n+1)n]^{1/3} \quad (6)$$

$$\frac{l}{n} < \frac{l_c}{n_k} \leq \frac{l+1}{n} \quad (7)$$

where, in atomic units, $n_k^2 = -\frac{Z^2}{2\varepsilon_k}$ and l_c is the classical value of the electronic angular momentum. These conditions permit to divide the phase space into adjacent nonoverlapping bins associated to the quantum numbers n, l by employing the Becker and McKellar^[25] binning method. In the present work, we have carried out the calculations for collisions with both targets, by including in the initial distribution only the trajectories with l_c fulfilling [Eqs. (6) and (7)] with $l=0$ for $H(2s)$ and with $l=1$ for the description of $H(2p)$ targets, i.e. averaged over magnetic quantum numbers.

Previous calculations on $C^{6+}, N^{7+} + H(n=2)$ collisions^[14] and $Be^{4+} + H(2s)$ ^[13] showed that the hydrogenic-CTMC treatment provides accurate ionization and total and n -resolved electron capture cross sections for $n \geq n_{\max}$ where n_{\max} is the most populated level of the ion $A^{(q-1)+}$ formed in the charge exchange reaction and, also provides accurate cross sections for excitation to $H(n)$ with $n > 3$. The microcanonical-CTMC treatment leads in general to more accurate electron capture cross sections into low-lying states, in

Table 1. Energies and weights of the hydrogenic initial distribution $H(n=2)$ (see [Eq. (5)]).

ε_j [hartree]	a_j
−0.1562500	0.3806820
−0.1351350	0.0851945
−0.1250000	0.1079310
−0.1162790	0.0912407
−0.1086960	0.0755748
−0.1020410	0.0765813
−0.0943396	0.0211866
−0.0877193	0.1616100

particular, for collisions with $H(1s)$ targets, as explained in detail in Refs. [14,21].

Once the initial distribution is constructed, the Hamilton equations are integrated for each nuclear trajectory $\mathbf{R}(t)$ from an initial time $t_{mi} = -500/v$ a.u. up to a final time of $t_{fin} = 1000/v$ a.u. The long collision time assures that the calculation correctly takes into account the Stark mixing in collisions with $H(n=2)$ targets. In order to disclose each inelastic process we determine the electron energies with respect to the target E_T and projectile E_P and, we apply the energy criteria at t_{fin} in which ionization takes place if $E_T, E_P > 0$, electron capture does if $E_T > 0$ and $E_P < 0$ and excitation takes place in the case of $E_T < 0$ and $E_P > 0$.

The corresponding ionization, electron capture and excitation probabilities are evaluated from the asymptotic values of the distribution functions,

$$P^{i,c,e}(v, b) = \int d\mathbf{r} \int d\mathbf{p} \rho^{i,c,e}(\mathbf{r}, \mathbf{p}; v, b, t_{fin}). \quad (8)$$

The integral cross sections are then calculated by integrating the transition probabilities over the impact parameter,

$$\sigma^{i,c,e}(v) = 2\pi \int_0^\infty db b P^{i,c,e}(v, b). \quad (9)$$

We can further define (n, l) levels within the capture and excitation channels by employing [Eqs. (6) and (7)] so as to obtain the transitions into the n and nl subshells. Thus, the capture density ρ^c (or excitation, using ρ^e) is divided into ρ_n^c and in turn in ρ_{nl}^c by including the trajectories in the corresponding boxes. State-selective probabilities and cross sections are determined by replacing ρ^c by ρ_n^c or ρ_{nl}^c in [Eq. (8)] and [Eq. (9)].

In our calculations we have considered both microcanonical and hydrogenic distributions and, we have verified that the convergence of the densities and probabilities with respect to the statistics and the integration time had been achieved.

Results and Discussion

Integral Cross Sections

Integral cross sections for the reactions Eqs. (1) and (2) have been computed for impact energies between 20 keV/u and 1000 keV/u. In order to obtain accurate results, we have

ensured the maximum impact parameter b_{\max} included is sufficiently large so that all inelastic processes vanish.

In Figure 1 we plot the energy dependence of the total ionization cross sections obtained using the CTMC method with both, the microcanonical and hydrogenic initial distributions, as described in previous section. The upper and lower panels correspond to the results for Be^{4+} scattering on $\text{H}(2s)$ and $\text{H}(2p)$, respectively. There is no experiment to compare with. We find very similar results between both targets with the maximum of the cross section around the projectile energy of 30 keV/u, reaching a slightly higher value of the ionization cross section in $\text{Be}^{4+} + \text{H}(2p)$ collisions that also shows a faster decrease for

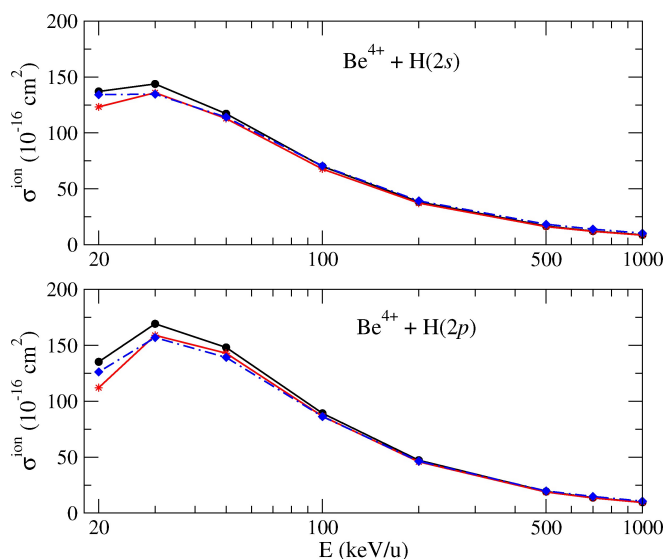


Figure 1. Ionization cross sections as functions of the impact energy in Be^{4+} collisions with $\text{H}(2s)$ (upper panel) and $\text{H}(2p)$ (lower panel) calculated with (—●—) h-CTMC and (---*---) m-CTMC compared to (---◆---) WP-CCC results from Antonio et al.^[12]

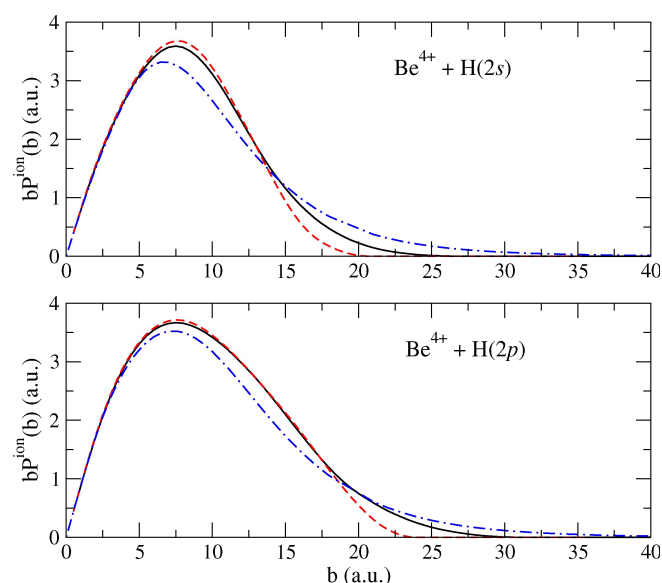


Figure 2. Ionization opacity functions $bP(b)$ as functions of the impact parameter b for an impact energy of 100 keV/u calculated with (—) h-CTMC and (---) m-CTMC and compared to (---) WP-CCC data from Antonio et al.^[12]

energies above the maximum. Classical ionization cross sections show a similar behaviour to the semiclassical wave-packet convergent close-coupling ionization cross sections.^[12] With regards to the threshold region ($E \lesssim 25$ keV/u), the cut-off of the radial microcanonical distribution limits the range of the impact parameter where the ionization process takes place yielding to smaller cross sections than those obtained in the hydrogenic-CTMC calculations which, in general, show a better agreement with the WP-CCC results. This effect, although considerably less perceptible, is also observed in Figure 2, where we have plotted the ionization opacity functions, i.e., the ionization probability distributions [Eq. (8)] multiplied by the impact parameter b , at the projectile energy $E = 100$ keV/u; in general, both classical calculations lead to similar $bP(b)$ values, and therefore similar total cross sections. To our knowledge, this is the first direct comparison between classical and semiclassical transition probabilities for $\text{Be}^{4+} + \text{H}(2s)$ and $\text{Be}^{4+} + \text{H}(2p)$ collisions, and shows that the good accord between the cross sections is not coincidental. Figure 3 displays total electron capture cross sections. Our computed m-CTMC cross sections are indistinguishable from the h-CTMC, and are in excellent agreement with WP-CCC calculations from Antonio et al.^[11] and with the 3-body CTMC results from Ziaeeian and Tökési^[15] for both excited targets across the entire energy domain, as well as, to the cross sections obtained with the numerical solution of the time-dependent Schrödinger equation (GTDSE)^[13] for $\text{Be}^{4+} + \text{H}(2s)$ collisions at the projectile energies 20 and 100 keV/u. However, we find a disagreement with the AOCC data from Igenbergs,^[9] which could be due to an overpopulation of the excited levels of Be^{3+} in that calculation, as previously found in Ref. [26]. We find that the electron capture cross section becomes considerably smaller than the ionization cross section for impact energies above 50 keV/u. To further analyze the accuracy of our classical calculations, we have plotted in Figure 4 the electron

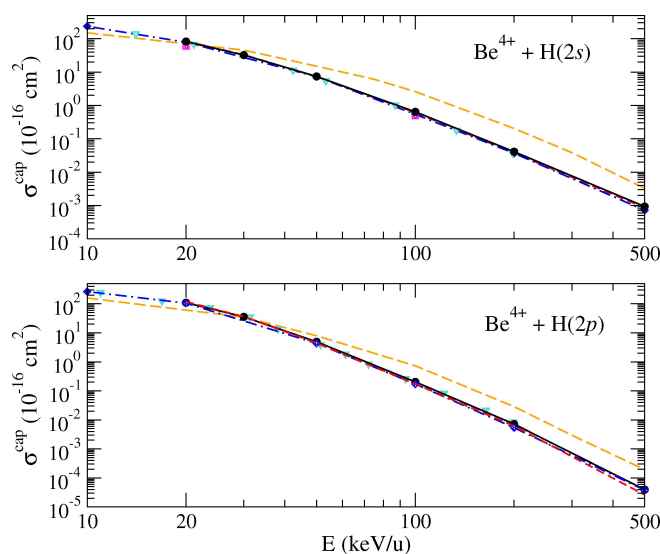


Figure 3. Electron capture cross sections as functions of the impact energy in Be^{4+} collisions with $\text{H}(2s)$ (upper panel) and $\text{H}(2p)$ (lower panel) calculated with the (—●—) h-CTMC and the (---*---) m-CTMC. Results from (■) GTDSE,^[13] (---◆---) WP-CCC,^[11] (▼) CTMC^[15] and (---▲---) AOCC.^[9]

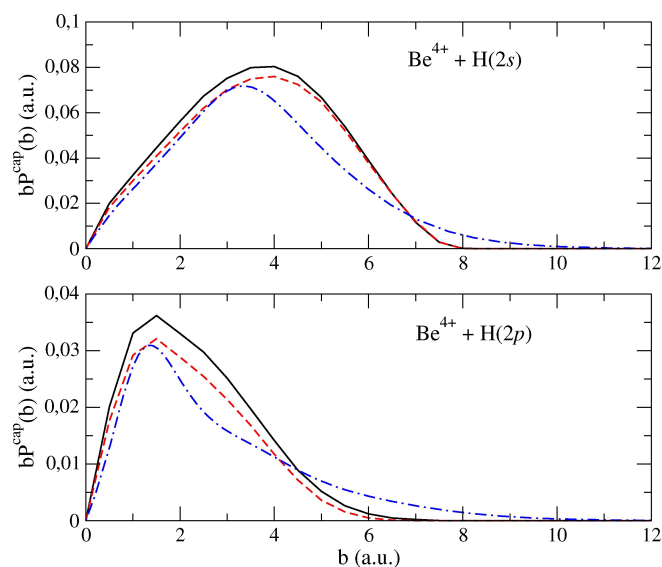


Figure 4. Electron capture opacity functions $bP^c(b)$ as functions of the impact parameter b for an impact energy of 100 keV/u calculated with (—) h-CTMC and (---) m-CTMC and compared to (···) WPCCC data from Antonio et al.^[11]

capture opacity function $bP^c(b)$ as functions of b for a projectile energy $E=100$ keV/u. Microcanonical and hydrogenic-CTMC calculations agree with each other and the agreement with the WP-CCC data^[11,12] is remarkably good despite the small value of the cross section at this collision energy. Moreover, different capture mechanisms are observed depending on the target state, in fact, the total capture cross section for $\text{Be}^{4+} + \text{H}(2p)$ reaction is one third of the corresponding capture cross section of $\text{Be}^{4+} + \text{H}(2s)$ at this collision energy. The peak positions and magnitudes in $bP^c(b)$ differ, showing a larger value of the maxima of the impact parameter in collisions with $\text{H}(2s)$ than in $\text{H}(2p)$ ($b_{\text{max}}=3.5$ a.u. and 1.5 a.u., respectively), which may explain the differences in the cross sections. This behaviour, which is observed in the semiclassical calculations, is probably due to the first (internal) maximum in the $\text{H}(2s)$ radial distribution which, at this relative ‘high’ projectile energy for the capture process, is the main contributor of electrons to the charge exchange process, and it is reproduced by the classical calculations.

Excitation and Electron Capture Partial n -resolved Cross Sections

Figure 5 displays cross sections for target excitation into the $n=4, 5, 6$ and 7 states as functions of projectile energy. The upper and lower panels correspond to the results for Be^{4+} collisions with $\text{H}(2s)$ and $\text{H}(2p)$, respectively. Excitation into $n=3$ states represents the dominant excitation channel over the entire energy range^[12,13] but we do not include this cross section because the CTMC does not provide an accurate excitation for reactions $n=2 \rightarrow n=3$. While m-CTMC data are underestimated due to the difficulty of the microcanonical distribution to reproduce the tail of the $\text{H}(n=2)$ quantal radial distribution, the h-CTMC calculation overestimates the $n=3$ excitation cross

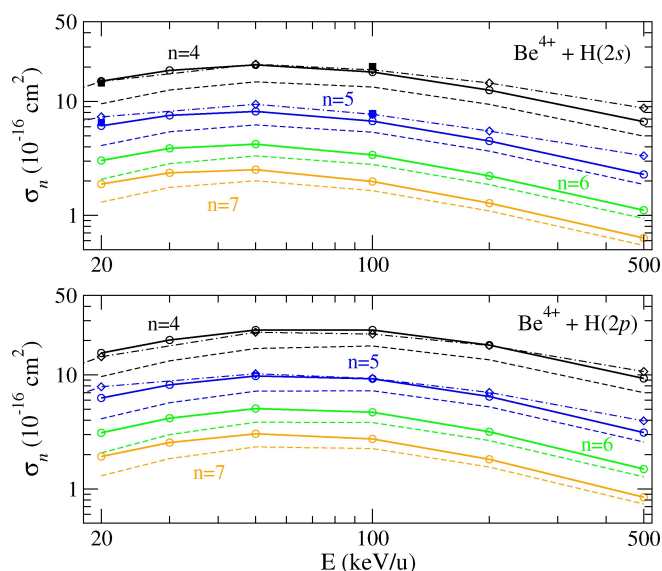


Figure 5. Cross sections for target excitation into $n=4, 5, 6$ and 7 states in Be^{4+} collisions with $\text{H}(2s)$ (upper panel) and $\text{H}(2p)$ (lower panel) calculated with (—○—) h-CTMC and (---○---) m-CTMC; (···◇···) WP-CCC data^[12] and (—■—) GTDSE results for $\text{H}(2s)$ ^[13] (upper panel).

sections because the electron trajectories with energy close to limit of the classical $n=2$ bin that yield an artificial increase of the excitation.^[13,27] On the other hand, h-CTMC provides reliable excitation cross sections into higher n levels,^[27] as can be observed in Figure 5 for excitations into $n=4$ and $n=5$ shells which show a reasonable agreement with those obtained GTDSE^[13] at 20 keV/u and 100 keV/u for $\text{Be}^{4+} + \text{H}(2s)$ collisions and, with the results obtained with WP-CCC^[12] calculations. However, the agreement seems to worsen from $E=200$ keV/u onwards with the semiclassical excitation sections being higher than the h-CTMC ones, and these differences are more noticeable in the case of $\text{H}(2s)$ targets. The transition to excited states, which involve outer electron trajectories, are generally underestimated at low and intermediate energies in the m-CTMC calculation, although the shape of both classical n -resolved excitation cross sections is similar and they show closer values to each other as n and the collision energy increase.

In Figure 6 we have plotted hydrogenic and microcanonical CTMC n partial electron capture cross sections for collisions with $\text{H}(2s)$ and $\text{H}(2p)$ targets compared to the semiclassical GTDSE^[13] and WP-CCC^[11] results. We observe, in general, a very good agreement for all n levels in the whole energy range. The differences in the n -resolved EC cross sections between the two targets are not significant, although those for $\text{Be}^{4+} + \text{H}(2p)$ show slightly larger values at higher n ($n=6, 7$) for $E < 50$ keV/u along with a more rapid fall as the energy increases than those for $\text{Be}^{4+} + \text{H}(2s)$ collisions. These results are completely consistent with the observations in Figure 3 since the n partial electron capture cross sections illustrated in Figure 6 are those corresponding to the dominant capture levels in this energy range.

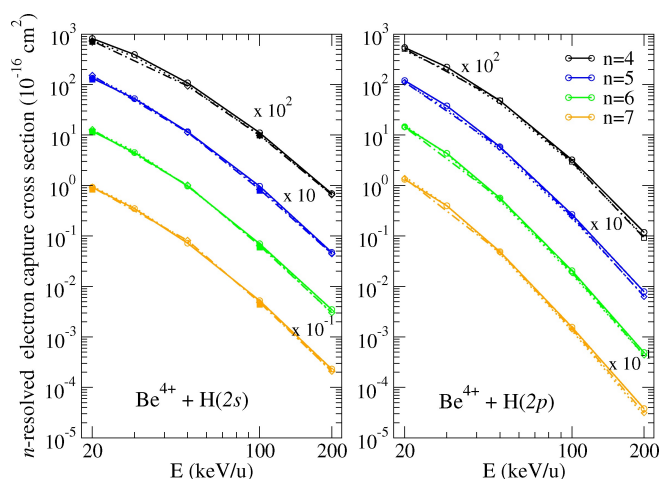


Figure 6. n -resolved electron capture into $n=4, 5, 6$ and 7 states cross sections for $\text{Be}^{4+} + \text{H}(2s)$ (left panel) and $\text{Be}^{4+} + \text{H}(2p)$ (right panel). Present calculation: (—○—) h-CTMC and (· · ·) m-CTMC shown alongside (—○—) WP-CCC calculations by Antonio et al.^[11] and (■) GTDSE results for $\text{H}(2s)$ ^[13] (left panel).

Conclusions

This work reports calculation of cross sections for ionization, electron capture and excitation processes in $\text{Be}^{4+} + \text{H}(2s)$, $\text{H}(2p)$ collisions in the intermediate energy range $20 \leq E \leq 1000$ keV/u. We have employed an impact parameter CTMC treatment and we have used two initial distributions, the standard microcanonical and the so-called hydrogenic one, whose spatial and momentum densities lie close to the quantal ones.

The present total electron capture cross sections are compared with previous AOCC results from Igenbergs^[6,9] and the recent classical 3-body CTMC^[15] and the semiclassical WP-CCC^[11] and GTDSE results.^[13] Total ionization cross sections are compared to those obtained using WPCCC approach by Antonio et al.^[12] At intermediate energies, CTMC ionization and electron capture cross sections present a good agreement with semiclassical results, as previously found for collisions with multicharged ions with $\text{H}(n=2)$ ^[14] and with $\text{H}(2s)$,^[13] and the basis for such a success in the electron transfer must be similar to that for the ionization and must rely on a dominance of two-body interactions in the capture process, as reasoned by Errea et al.^[21] With regards to the target excitation process, we find that the use of a microcanonical initial distribution leads to an underestimation of the n partial excitation cross sections but the implementation of an improved hydrogenic initial distribution redresses this yielding to a better description of the excitation into $\text{H}(n \geq 4)$ in collisions with $\text{H}(2s)$ and $\text{H}(2p)$ targets, showing a good agreement with the semiclassical results available.^[12,13] This supports the use of the h-CTMC method for the determination of excitation cross sections into high n -lying excited levels.

The comparative study of Be^{4+} ions in collision with $2s$ and $2p$ hydrogen targets reveals the differences in the studied inelastic processes are not remarkable.

This performance of CTMC calculations is very encouraging, since they are considerably simpler than ab initio close-coupling treatments and they are free from the problems of discrimination between capture, excitation and ionization fluxes inherent in the above-mentioned semiclassical approaches.

Acknowledgements

I would like to thank to L. Méndez for fruitful discussions. This work has been partially supported by the Ministerio de Economía, Industria y Competitividad (Spain), project no. FIS2017-84684-R. This work was a part of the Coordinated Research Project carried out under the sponsorship of the International Atomic Energy Agency, Data for Atomic Processes of Neutral Beams in Fusion Plasma.

Conflict of Interests

The author declare no conflict of interest.

Data Availability Statement

The data that support the findings of this study are available from the corresponding author upon reasonable request.

Keywords: integral cross sections · ion-atom collisions · highly charged ions · gas-phase chemistry · Monte-Carlo calculations

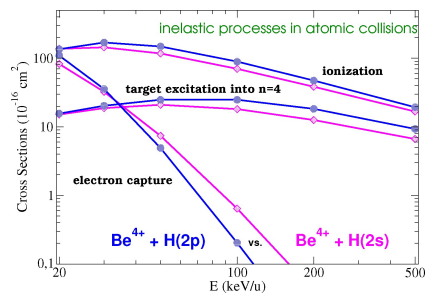
- [1] R. C. Isler, *Plasma Phys. Controlled Fusion* **1994**, 36, 171.
- [2] R. McDermott, R. Dux, F. Guzman, T. Putterich, R. Fischer, A. Kappatou, the ASDEX Upgrade Team, *Nucl. Fusion* **2021**, 61, 016019.
- [3] R. K. Janev, J. J. Smith, *At. Plasma-Mater. Interact. Data Fusion* **1993**, 4, 1.
- [4] R. C. Isler, R. E. Olson, *Phys. Rev. A* **1988**, 37, 3399.
- [5] R. Hoekstra, H. Anderson, F. W. Blik, M. von Hellerman, C. F. Maggi, R. E. Olson, H. P. Summers, *Plasma Phys. Controlled Fusion* **1998**, 40, 1541.
- [6] K. Igenbergs, J. Schweinzer, A. Veiter, L. Perneczky, E. Frühwirth, M. Wallerberger, R. E. Olson, F. Aumayr, *J. Phys. B: At. Mol. Opt. Phys.* **2012**, 45, 065203.
- [7] L. F. Errea, C. Harel, H. Jouin, L. Méndez, B. Pons, A. Riera, *J. Phys. B: At. Mol. Opt. Phys.* **1998**, 31, 3527.
- [8] K. Igenbergs, J. Schweinzer, F. Aumayr, *J. Phys. B: At. Mol. Opt. Phys.* **2009**, 42, 235206.
- [9] K. Igenbergs, Ph.D. thesis, Vienna University of Technology, Vienna, Austria **2011**.
- [10] N. W. Antonio, C. T. Plowman, I. B. Abdurakhmanov, I. Bray, A. S. Kadyrov, *J. Phys. B: At. Mol. Opt. Phys.* **2021**, 54, 175201.
- [11] N. W. Antonio, C. T. Plowman, I. B. Abdurakhmanov, I. Bray, A. S. Kadyrov, *Phys. Rev. A* **2022**, 106, 012822.
- [12] N. W. Antonio, C. T. Plowman, I. B. Abdurakhmanov, I. Bray, A. S. Kadyrov, *Atom* **2022**, 10, 137.
- [13] A. Jorge, C. Illescas, L. Méndez, *Phys. Rev. A* **2022**, 105, 012811.
- [14] A. Jorge, L. F. Errea, C. Illescas, L. Méndez, *Eur. Phys. J. D* **2014**, 2014, 227.
- [15] I. Ziaei, K. Tökési, *Eur. Phys. J. D* **2021**, 2021, 138.
- [16] R. Abrines, I. C. Percival, *Proc. Phys. Soc.* **1966**, 88, 861.
- [17] B. H. Bransden, M. H. C. McDowell, *Charge Exchange and the Theory of Ion-Atom Collisions*, Oxford, Clarendon **1992**.

- [18] N. G. D. Eichenauer, W. Scheid, *J. Phys. B: At. Mol. Opt. Phys.* **1981**, *14*, 3929.
- [19] J. S. Cohen, *J. Phys. B: At. Mol. Opt. Phys.* **1985**, *18*, 1759.
- [20] C. Illescas, A. Riera, *Phys. Rev. A* **1999**, *60*, 4546.
- [21] L. F. Errea, C. Illescas, L. Méndez, B. Pons, A. Riera, J. Suárez, *Phys. Rev. A* **2004**, *70*, 52713.
- [22] R. E. Olson, *Phys. Rev. A* **1981**, *24*, 1726.
- [23] C. Illescas, I. Rabadán, A. Riera, *J. Phys. B: At. Mol. Opt. Phys.* **1997**, *30*, 1765.
- [24] D. J. W. Hardie, R. E. Olson, *J. Phys. B: At. Mol. Phys.* **1983**, *16*, 1983.
- [25] R. L. Becker, A. D. MacKellar, *J. Phys. B: At. Mol. Phys.* **1984**, *17*, 3923.
- [26] A. Jorge, J. Suárez, C. Illescas, L. F. Errea, L. Méndez, *Phys. Rev. A* **2016**, *94*, 032707.
- [27] J. Suárez, F. Guzmán, B. Pons, L. F. Errea, *J. Phys. B: At. Mol. Opt. Phys.* **2013**, *46*, 095701.

Manuscript received: April 28, 2023
Revised manuscript received: July 19, 2023
Accepted manuscript online: July 21, 2023
Version of record online: ■■, ■■

RESEARCH ARTICLE

Collisions between (excited) hydrogen atoms and beryllium impurity ions are expected to occur inside fusion reactors and the cross sections of all inelastic processes are then needed. A comparative study of H(2s) and H(2p) targets in collision with Be^{4+} ions at fusion-relevant energies is presented.



Dr. C. Illescas*

1 – 7

Calculation of Ionization, Excitation and Electron Capture Cross Sections for $\text{Be}^{4+} + \text{H}(2s, 2p)$ Collisions

Special
Collection